$12CaO.7Al_2O_3$ ceramic: A review of the electronic and optoelectronic applications in display devices

Elnaz Feizi and Asim K. Ray*

Centre for Materials Research, Queen Mary, University of London, Mile End Road, London E1 4NS, UK

Keywords: C12A7, FED, LED, FET, phosphor, emitter, conductivity

Abstract

The alumina-based compound, $12CaO.7Al_2O_3$, is a ceramic material with a unique cage-like lattice. Such a structure has enabled scientists to extract various new characteristics from this compound, most of which were unknown until quite recently. This compound has the ability to incorporate different anionic species and even electrons to the empty space inside its cages, thereby changing from an insulator into a conductive oxide. The cage walls can also incorporate different rare earth phosphor elements producing an oxide-based phosphor. All these characteristics are obtained without a significant change in the structure of the lattice. It is, therefore, reasonable to expect that this compound will receive attention as a potential material for display applications. This review article presents recent investigations into the application of $12CaO.7Al_2O_3$ ceramic in various display devices, the challenges, opportunities and possible areas of future investigation into the development of this naturally abundant and environmental friendly material in the field of display.

* Present address: Institute of Materials and Manufacturing, Brunel University London, Uxbridge, Middlesex UB8 3PH, UK

This article has been accepted for publication in a future issue of this journal, but has not been fully edited. Content may change prior to final publication. Citation information: DOI 10.1109/JDT.2015.2496588, Journal of Display Technology

1. Introduction

Display technology has been around for many years with widespread applications in the production of visual-based devices, among which television, computer monitors and mobile phone screens are the most attractive devices in terms of public demand. This technology, however, is still growing and the constant development of display devices is requisite with the main focus on the improvement of efficiency and picture quality, reducing weight and power consumption, selection of environmentally friendly/abundant materials, and the production of more advanced *futuristic* devices such as 3-dimentional, flexible and transparent displays.

Such constant need for development of optimised display devices has led to new and otherwise unknown materials being investigated as substitutes for conventional materials, such as transparent conductive oxides and semiconductors as well as materials with unique crystal structures and characteristics.

The oxide-based compound, $12CaO.7Al_2O_3$, also named C12A7, has been used for several years as one of the constituents of cement. It has been recognised, however, as an attractive candidate for various electronic and optoelectronic applications due to its unique structure [1]. The unit cell of C12A7 is comprised of two $12CaO.7Al_2O_3$ molecules [2] with the stoichiometric chemical composition represented as $[Ca_{24}Al_{28}O_{64}]^{4+}.2O^{2-}$. $[Ca_{24}Al_{28}O_{64}]^{4+}$ is the framework with a mean positive charge of +1/3 and forms a cage-like structure [3, 4]. The cage structure of C12A7 is shown in figure 1. Each unit cell contains 12 cages and 2 out of 12 cages are randomly incorporated with O^{2-} ions, also known as extraframework ions, in order to neutralize the extra positive charge of the cell. The empty cages have a concentration of approximately 5×10^{21} cm^{-3}, each with an empty space of around 0.6 nm in diameter [5, 6]. In practice, various types of anionic species, e.g. OH^-, H^-, O^-, and electrons, can be distributed inside the lattice depending on the processing techniques. The material exhibits different physical properties depending on the type of incorporated anions without a significant change in the structure of the lattice. Several techniques have been developed in order to incorporate electrons into the structure of C12A7. The values of conductivities and electron concentrations for some of these methods are given in figure 2. A heat treatment under vacuum and in presence of Ca [7] or Ti [8] metal is a widely known method for single crystalline bulk. The heat treatment of C12A7 thin films in a reducing atmosphere of H_2/N_2 can incorporate H^- ions into the cage structure of C12A7, which are converted to e^- upon UV irradiation with moderate electrical conductivities (up to

This article has been accepted for publication in a future issue of this journal, but has not been fully edited. Content may change prior to final publication. Citation information: DOI 10.1109/JDT.2015.2496588, Journal of Display Technology

~0.5S.cm^{-1}) [9]. Alternatively, a heat treatment under vacuum with a thin layer of oxygen-deficient amorphous C12A7 deposited on top of the polycrystalline film can produce electrical conductivities of up to 800 $S\,cm^{-1}$ [10]. A two-step melt solidification technique in a carbon crucible is ideal for the production of conductive polycrystalline bulk [11].

The optical transparency, chemical stability in air and at room temperature, ionic and electronic conductivity, and natural abundance of this compound are highly desirable and the main reasons for the special attention it has been receiving as a potential material for display applications. Additionally, doping the C12A7 framework with phosphor ions during material synthesis has proven to be effective in the production of C12A7 phosphors which makes it even more interesting as a potential display material. This article reviews some of the investigations that have been made to date in exploring the unique characteristics of C12A7 compound in the field of display devices as well as current problems and voids in the process of device fabrication and performance. Some suggestions and ideas for future investigations have also been provided that can further enhance the possibility of this unique material to find its place as a conventional display material.

2. Dual functionality of C12A7 in field emission display

Field emission displays (FEDs) are widely considered in flat panel display applications due to several attractive qualities, such as wide viewing angle, slim panels, high contrast ratio, quick response, low weight, inertness to variations of temperature and power efficiency [12]. The main challenges in the fabrication of FED devices are the choices of an efficient electron emitter and suitable phosphors with high brightness levels and long lifetimes. C12A7 has recently attracted considerable attention as both an electron emitter and phosphor for FED applications. It is, therefore, considered as a potential material with dual functionality in the field of FEDs.

2.1 C12A7 electron emitter in field emission display

Several materials have been investigated as electron emitters for field emission display applications, such as metals (e.g. W and Mo), organic electron emitting materials (electrides) and carbon-based structures and nanostructures. Emitters with narrow elongated shapes and sharp tips can enhance the local electric field and reduce the turn-on

This article has been accepted for publication in a future issue of this journal, but has not been fully edited. Content may change prior to final publication. Citation information: DOI 10.1109/JDT.2015.2496588, Journal of Display Technology

field. Nanostructures with high aspect ratios, such as nanotubes, have been receiving special attention as field emitters [13]. In addition to good conductivity, low work function and high aspect ratio geometry, the emitter material must resist deformation due to high temperatures, since the electron emission can cause heating of the emitter tip, especially at high emission currents, even though the emission starts at room temperature [14].

Electron incorporated C12A7 exhibits superior characteristics compared to previously known electron emitting materials. A work function of ~3.7 eV has been determined for conductive C12A7, while the apparent work function based on field emission measurements is as low as ~0.6 eV [15]; much lower than that reported for carbon nanotubes [16]. The oxidization of the C12A7 surface and formation of a thin semiconductive surface layer is responsible for the dramatic decrease in the value of the apparent work function via the band bending effect, which is beneficial in order to improve the efficiency of cold emission [15]. Additionally, the chemical stability of C12A7 in air or a humid environment at room temperature as well as considerably higher emission current makes it superior to organic electrides [17, 18].

The schematic illustration of a typical field emission display with conductive C12A7 as the electron emitter is depicted in figure 3. A single crystal C12A7:e^- with a flat surface can produce an emission current of 22 μAcm^{-2} at an extraction voltage of ~2100 V. The extraction voltage can be reduced to almost half if the emitter surface is roughened [15]. It is expected for modified surface geometries to exhibit even higher emission currents and reduce the extraction voltage. Therefore, the development of new processing techniques resulting in the fabrication of sharp elongated C12A7 emitters is indispensable.

It is worth comparing the electronic and field emission properties of the single crystalline and polycrystalline material. The highest electrical conductivity obtained in the electron incorporated C12A7 depends on the crystal structure as well as the fabrication technique [15]. For instance, the C12A7:e^- single crystal formed via heat treatment of the single crystalline material in presence of Ca metal, gives a typical electrical conductivity of ~100 $S.cm^{-1}$ [3], while the polycrystalline material exhibits an electrical conductivity of almost two orders of magnitude lower (~5 Scm^{-1} for melt-solidification process [18]). However, it is interesting to know that both single crystalline and polycrystalline bulks give similar electron mobilties of $\sim 0.1\, cm^2V^{-1}s^{-1}$ [18], which is mainly due to large grains formed in the polycrystalline electride. On the other hand, the reducing heat treatment of C12A7

This article has been accepted for publication in a future issue of this journal, but has not been fully edited. Content may change prior to final publication. Citation information: DOI 10.1109/JDT.2015.2496588, Journal of Display Technology

single crystals in presence of Ti metal as a substitute for Ca, results in a significant improvement of conductivity (up to 1500 Scm^{-1}) and drift mobility ($\sim 4\ cm^2V^{-1}s^{-1}$) [19].

A comparison between the emission current-voltage characteristics of single crystalline and polycrystalline C12A7:e^- is given in figure 4. The emission current obtained from a polycrystalline bulk is lower than that of a single crystal and a higher extraction voltage is required for the electron emission to start. For instance, for two flat C12A7:e^- emitters working under similar testing apparatus, the emission current of single crystalline emitter reaches 22 μAcm^{-1} at 2100 V [15], while the value of emission current is almost half (12 $\mu A.cm^{-1}$) at a higher extraction voltage of 2400 V [11]. The emission current durability of C12A7 electride is also a determining factor for practical applications in field emission displays and should be studied more thoroughly, although it has been previously reported that the emission current is stable over the duration of one day [11].

Conductive C12A7 thin films can also be considered as electron emitters. The heat treatment of an insulating polycrystalline thin film with an amorphous C12A7 over-layer can produce a conductive thin film with excellent electrical conductivity of 800 $S.cm^{-1}$ and a maximum Hall mobility of 2.5 $cm^2V^{-1}s^{-1}$. An increase in the film thickness can enhance the electrical conductivity due to an increase in the carrier mobility. For instance, a conductivity of ~450 Scm^{-1} is obtained from a film with 150 nm thickness, while a conductivity of ~800 Scm^{-1} is achieved for a film thickness of 400 nm or more. Therefore, it is possible to regulate the value of electronic properties by adjusting the film thickness [20].

Efforts have been made in order to further improve the electrical properties of C12A7:e^- thin films by fabricating epitaxial layers. Although the carrier concentration and Hall mobility is improved in the epitaxial film compared to non-oriented film, the improvement is only significant at low temperatures and the difference in electrical properties is reduced as the temperature is increased towards room temperature [21].

2.2 C12A7 phosphors in field emission display

Materials with long lasting phosphorescent properties have a great potential to be used in display devices [22]. Rare-earth ions with emission properties, such as Ce, Tb, Eu and Er, can act as active centres for luminescence [23, 24].

This article has been accepted for publication in a future issue of this journal, but has not been fully edited. Content may change prior to final publication. Citation information: DOI 10.1109/JDT.2015.2496588, Journal of Display Technology

In addition to high emission efficiency [25], thermal and chromatic stability and long lifetime [26], the phosphor used in FEDs needs to be electrically conductive in order to prevent charge accumulation on the phosphor surface [12, 27].

Sulfide-based compounds have high efficiency and good electrical conductivity, however sulphur is volatile, which is the main drawback for the application of these compounds as phosphors in field emission displays [12]. Oxide-based materials, such as aluminates [24], exhibit good thermal and chemical stabilities in addition to superior colour richness. Most oxide-based compounds, however, are insulators and are not stable under electron beam irradiation. Although efforts have been made to increase the conductivity of oxide compounds via coating or mixing with transparent conductive oxides, such as SnO_2, In_2O_3 or ZnO, the problem of instability under electron bombardment requires further investigations. Furthermore, the process of coating/mixing is complicated and expensive [12].

C12A7 is proven to be a great host for rare-earth phosphors with the possibility to be converted into a semiconductor. For instance, wide band gap semiconductors are especially suitable hosts for Er doping, since a large band gap is effective in reducing the thermal quenching effects of Er^{3+} ions [28]. C12A7 is known to have a wider band gap compared to alternative potential hosts such as Si [23], GaN, ZnO and TiO_2 [23, 28]. In addition, the incorporation of random cages with O^{2-} ions reduces the local symmetry of the crystal field around the framework Ca and Al sites, which can enhance the photoluminescence (PL) of Er^{3+} ions. The substitution of entrapped O^{2-} ions with other ions such as H^- and O^- or electrons can further develop the potential applications of Er doped C12A7 in the optoelectronic field [28].

Er^{3+} doping of C12A7 produces multiplet green and red emissions in the visible wavelength region with the intensity of green emission being stronger than that of the red emission [28]. The major green emission bands are positioned at 525 and 545 nm respectively under 488 nm excitation. The emission intensity is strongly dependent upon the concentration of the dopant [23], and therefore, can be tuned by adjusting the dopant concentration. A comparison between the photoluminescence of C12A7:Er^{3+} and the commercial photoluminescent compound GaN:Er^{3+} shows a sharper emission for C12A7:Er^{3+}. Such a sharp multiplet emission of C12A7:Er^{3+} is the result of a stronger field effect induced by C12A7 lattice compared to GaN [28].

Ce^{3+} doped C12A7 has also been considered as a potential blue phosphor. The doped material shows a broad luminescence peak positioned at ~413 nm under ~270 nm

This article has been accepted for publication in a future issue of this journal, but has not been fully edited. Content may change prior to final publication. Citation information: DOI 10.1109/JDT.2015.2496588, Journal of Display Technology

excitation, which is quite different from the typical doublet luminescence of Ce^{3+} dopants. The extra positive charge of the Ce^{3+} is compensated for with negatively-charged encaged species such as O^{2-} and electrons. If the extra positive charge of the lattice due to doping is not completely neutralised, the C12A7 structure can become unstable which favours the formation of other more stable phases. In other words, the presence of phases other than doped C12A7 might be inevitable [24].

Double doping with two different phosphor rare earth ions gives the possibility of emission colour tuning as well as improvement of photoluminescence and cathodoluminescence (CL) properties due to efficient energy transfer from one type of dopant to the other. Such behaviour is observed with Ce^{3+} and Tb^{3+} phosphors [27]. The co-doping of C12A7 with Ce^{3+}, Tb^{3+} results in a green emission with the major emission peak positioned at 543 nm under UV light excitation [27, 29]. In addition, the modification of the processing technique can produce a C12A7 green phosphor which is electrically conductive. It is worth mentioning, however, that the fabrication of the conductive C12A7 phosphor is accompanied by some technical problems such as long hours of heat treatment and the inevitable formation of secondary phases.

C12A7:Ce^{3+}, Tb^{3+} is produced via solid state reaction followed by a subsequent heat treatment in a reducing atmosphere of H_2/N_2, which can incorporate H^- ions into the cages of C12A7 and convert the tetravalent dopants to their trivalent states. Electrons are then incorporated into the material upon UV light illumination [12].

If the concentration of Ce^{3+} is high enough, $CaCeAl_3O_7$ is preferentially formed along with minor amounts of $CaAl_2O_4$, which is the product of C12A7 decomposition. The formation of $CaCeAl_3O_7$ secondary phase is claimed to be beneficial in terms of improving PL and CL under low voltages (as low as 800 V) [27] as long as H^- incorporated C12A7 remains as the main phase. The compound also exhibits short decay times compared to commercial phosphors which can improve the display quality in fast moving pictures and make it suitable for FED applications [12].

Eu^{3+} doped C12A7 is a red phosphor with the peaks locating at 586 and 616 nm under UV excitation within the wavelength range of 570-630 nm [22, 27]. Subsequent heat treatment of the phosphor in various atmospheres/ temperatures has proven to change the luminescence characteristics of C12A7:Eu phosphors mainly due to the alteration of the type and concentration of encaged anions as well as the oxidation state of the phosphor dopants.

This article has been accepted for publication in a future issue of this journal, but has not been fully edited. Content may change prior to final publication. Citation information: DOI 10.1109/JDT.2015.2496588, Journal of Display Technology

The annealing treatment of C12A7:Eu^{3+} in a reducing atmosphere of H_2/ N_2 results in a significant reduction of red emission along with the detection of blue emission, thereby converting the material from a red phosphor to a blue phosphor. The change in colour and intensity of the emission can be attributed to a number of factors including the amount of active centres and the type and concentration of encaged anions in C12A7. The reducing heat treatment results in the incorporation of H^- and OH^- ions as substitutes for encaged O^{2-} [27]. In addition, the Eu^{3+} dopant is partly reduced to Eu^{2+}. As a result, the red emission of Eu^{3+} is significantly reduced and a blue emission belonging to Eu^{2+} in the 400-500 nm region occurs, exhibiting a broad peak with maximum intensity at ~444 nm [22, 27]. A subsequent reverse annealing of the reduced compound in air results in the enhancement of both red and blue emission intensities with an overall improvement in the blue emission of the phosphor [27]. The colour tuning of C12A7: Eu^{3+}, Eu^{2+} can be extremely beneficial in production of phosphor with the desired emission colour and intensity for FED applications.

3. C12A7 channel in field –effect transistors

One of the main components of a field effect transistor (FET) is the semiconductive channel layer. The choice of a suitable channel material critically determines the performance and efficiency of the device. The controllability of the channel carrier density and the electric potential via an external electric field are essential for the proper function of the transistor. Additionally, the channel should exhibit a high field-effect mobility. The quality of the channel layer and the interfaces with the gate insulator and electrodes as well as the choice of a good gate insulator material with high dielectric constant are contributing factors affecting the field-effect mobility [30]. In an efficient FET device, the source-to-drain current shows a pinch-off and a good drain current saturation with the increase in the source- drain voltage [30, 31]. A low off-current and high on-off current ratios, which result in normally-off characteristics of the device, as well as a small photo-response, are also desired [30].

Transparent oxide semiconductors, such as ITO, SnO_2 and ZnO, have attracted attention as potential channel materials in transparent field-effect transistors (TFETs) as substitutes for Si-based devices [31-33]. Advantages of these semiconductors include optical transparency and high voltage and temperature tolerance. In addition, the performance of the TFET device is not adversely affected by visible light irradiation. However, conventional

This article has been accepted for publication in a future issue of this journal, but has not been fully edited. Content may change prior to final publication. Citation information: DOI 10.1109/JDT.2015.2496588, Journal of Display Technology

transparent oxide semiconductors used in TFETs, such as ZnO, exhibit large off-current and normally-on characteristics mostly due to the difficulty in controlling the carrier concentration down to intrinsic levels during the semiconductor preparation. Although polycrystalline ZnO shows high on-off current ratios of the order of 10^7, the field effect mobility is very low (0.35-0.45 $cm^2.V^{-1}.s^{-1}$) [34] due to the limiting effect of the grain boundary potential barriers [30, 33]. It is not easy to regulate the carrier density without doping and carrier doping is difficult for large band gap semiconductors [33]. The field-effect mobility of ZnO-based transistors is generally inferior to single crystalline Si-based devices and only comparable to amorphous Si and organic transistors [34]. Organic compounds have been considered as substitutes for silicon mostly due to lower cost, especially if the device fabrication is solution based [35]. However, as mentioned previously, organic materials exhibit low performance and stability in environmental conditions [36].

C12A7 has proven to be an excellent conductive oxide with unique electrical and chemical properties. The concentration of incorporated electrons in the material varies according to the method of incorporation and can be controlled over a range of $<10^{17}$ to 2×10^{21} cm^{-3}. Although the electronic structure and carrier transport mechanism in C12A7 is quite different from other conventional semiconductors, it is possible to regulate the carrier generation via an external electric field, similar to other conventional semiconductive channel materials [17].

Both single crystalline bulk and polycrystalline thin film of C12A7 have been considered as channels in an FET device. In the case of the C12A7 thin film channel, the semiconducting film on MgO single crystalline substrate is used as the channel material. Figure 5 shows the configuration of FETs based on single crystalline bulk and polycrystalline thin film of C12A7. There are, however, a number of challenges to be addressed in the application of C12A7 semiconductor as channel in FETs.

The carrier generation in C12A7:e^- can be regulated by an external electric field as long as the concentrations of other anionic species are kept to a minimum level during the channel and device fabrication. The co-existence of electrons with other anionic species, such as O^{2-}, in C12A7 semiconductor is requisite for the structural stability of the material. However, such a presence can also be disadvantageous in a field-effect device where electronic potential alteration is required. Each anion species forms its own electronic levels in the fundamental band gap of the C12A7 framework, which can act as barriers for the Fermi level, hence preventing the device from functioning.

This article has been accepted for publication in a future issue of this journal, but has not been fully edited. Content may change prior to final publication. Citation information: DOI 10.1109/JDT.2015.2496588, Journal of Display Technology

Another challenge in the fabrication of C12A7-based FETs is the formation of an Ohmic contact between the channel and conventional source/drain electrodes due to the relatively low work function of C12A7 with respect to the electrodes. The C12A7:e^--Pt contact shows the closest behaviour to the linear current-voltage characteristics of an Ohmic contact. In addition, an annealing treatment of the contact at temperatures higher than 300^oC in vacuum reduces the contact resistance of the interface, although such treatment cannot eliminate the effect of Schottky barriers completely. In addition, this method is not applicable to thin films [17].

The leakage current through the gate insulator of a C12A7-based transistor is also a major factor, with adverse effect on the device performance. Although the leakage current can be reduced by increasing the thickness of the gate insulator, the gate capacitance and carrier concentration are decreased as a result. Therefore, the choice of a gate insulator material with a high dielectric constant is very important in order to maintain a high gate capacitance. Y_2O_3 with a large dielectric constant of $\sim 16\varepsilon_o$ is suggested [17]. The high surface roughness of the C12A7 channel also increases the leakage current of the gate. Therefore, decreasing the surface roughness of the channel can reduce the leakage current through the gate so that a thick insulator is no longer required.

The single crystalline C12A7-based device exhibits an apparent field-effect mobility and on-off ratio of $\sim 0.08\ cm^2V^{-1}.s^{-1}$ and ~10 respectively. Although, the on- current and field- effect mobility of the polycrystalline C12A7 thin film is lower than those of single crystal, the on-off current ratio is significantly improved. Since the current leakage mostly occurs in the deep regions of the channel, the thin layer of C12A7 film seems to be advantageous in reducing the drain-source leakage current [17].

Additionally, the drift mobility of a C12A7-based device is low compared to conventional channel semiconductors and the main problems of finding a proper electrode material, which can form an Ohmic contact with C12A7 channel, as well as reducing the surface roughness of the channel are yet to be resolved.

4. C12A7 in lighting

4.1 C12A7 phosphor in white light emitting diodes

Light emitting devices, such as white light emitting diodes (LEDs), have attracted considerable attention as substitutes for incandescent and fluorescent lamps [26] due to

This article has been accepted for publication in a future issue of this journal, but has not been fully edited. Content may change prior to final publication. Citation information: DOI 10.1109/JDT.2015.2496588, Journal of Display Technology

their longer life time, high luminescence efficiency and energy saving [26, 29, 37]. In order to produce white light, a blue LED chip as a pump source combined with green and red phosphors or a UV LED chip combined with all three basic colours of blue, red and green phosphors are used [38]. Phosphor materials suitable for this purpose should have high emission in the visible region and high absorption in the UV or blue range.

Various types of doped C12A7 phosphor can emit primary colours upon UV excitation. Table 1 summarizes several C12A7 phosphors which can be used in near-UV white (350-420 nm) LEDs. In addition to the popular methods of white light production mentioned above, it is possible to produce white light via generation of blue and yellow colours under UV excitation.C12A7 doped with rare earth Dy^{3+} ion emits white light by mixing blue and yellow emissions under UV excitation with blue and yellow emission bands at 480 and 571 nm respectively.

The main drawback in the production of white light via Dy^{3+} doping is that the emission intensity of yellow light is generally weaker than that of blue emission. The Dy^{3+} doped C12A7, however, gives higher yellow emission intensity with much higher yellow to blue emission ratio than is typically observed from other Dy^{3+} doped hosts. The reason can be attributed to the low symmetry of the Dy^{3+} local states in C12A7 crystal [26].

The vacuum annealing of the doped C12A7 at 900 ^{o}C improves the emission intensity of Dy^{3+} in both blue and yellow regions with no change in the yellow to blue intensity ratio. Furthermore, the thermal and chromatic stability of the Dy^{3+} doped C12A7 phosphor is proven [26]. The Dy^{3+} doped C12A7 gives a yellowish white light emission, which is some distance from the ideal white light emission.

Double doping of C12A7 with Ce^{3+} and Dy^{3+}, on the other hand, results in white light emission close to ideal white light, which is much improved compared to singly doped C12A7:Dy^{3+} with a yellowish white light emission. Figure 6 gives a comparison between the emission spectrum of Ce^{3+}, Dy^{3+} co-doped C12A7 with that of Dy^{3+} doped material. The overlap between the emission band of Ce^{3+} and excitation wavelength region of Dy^{3+} causes an efficient energy transfer from Ce^{3+} to Dy^{3+}. When excited via UV light, the material exhibits a bluish white emission due to emission of Ce^{3+} at 430 nm and emission of Dy^{3+} at 476 and 576 nm. As the concentration of Ce^{3+} dopant is increased, the PL of Dy^{3+} is improved mainly due to the efficient energy transfer from Ce^{3+} to Dy^{3+} [25]. It is also possible to introduce electrons into doped C12A7 via heat treatment of C12A7 in a reducing atmosphere containing H_2 followed by UV irradiation. An electrical conductivity

This article has been accepted for publication in a future issue of this journal, but has not been fully edited. Content may change prior to final publication. Citation information: DOI 10.1109/JDT.2015.2496588, Journal of Display Technology

of ~0.01 $S.cm^{-1}$ can be reached, which is considerably higher than the value of 5.2 $\mu S.cm^{-1}$ reported for Eu^{3+} doped Y_2O_3 phosphor coated with In_2O_3 [25].

It is noteworthy that the UV illumination of doped C12A7 slightly affects the emission properties of Dy^{3+}. The overall emission intensity decreases after UV irradiation and the intensity of yellow emission increases with respect to blue emission. The CL of the co-doped C12A7 follows similar behaviour before and after UV irradiation, although the effect of energy transfer is less apparent.

4.2 C12A7 cathode in organic light emitting diodes

One of the main challenges in improving the performance and lifetime of organic light emitting diodes (OLEDs) is to overcome the carrier injection barrier forming in electrode-organic layer interfaces [39]. Conventional organic electron transport materials have electron affinities much smaller than the work function of typical cathode materials. This difference yields a high electron injection barrier at cathode/ organic interface, which in turn increases the operation voltage and decreases the long term stability [40]. Since most organic semiconductors are p-type with lower electron mobility compared to hole mobility, the emission efficiency is determined by the number of injected electrons. The hole injection barrier at anode-hole transport material is smaller, and therefore, less problematic; while the electron injection barrier voltage in the cathode-organic layer interface can reach to more than 1 eV [39]. Therefore, lowering the electron injection barrier is the solution to decreasing the operating voltage and increasing the emission efficiency of the device. In order to reduce the electron injection barrier, materials with low work functions, such as Na, Mg and Ca, are required. However, these metals do not possess the required chemical stability [40] and their application as cathode for OLEDs is impractical.

Electron incorporated C12A7 is an alternative cathode material with chemical stability and a low work function comparable to the electron affinity of the electron transport material [40, 41]. Since C12A7 does not react with organic materials, it can be a good candidate as an electrode material for organic based devices. The small barrier along with the chemical stability of C12A7:e^- cathode improves the efficiency of the OLED substantially. Other advantages include lower operating voltage, cost effectiveness and longer life time of the device [41]. On the other hand, the application of C12A7:e^- as cathode for OLEDs brings up some challenges to overcome in the design and fabrication of the device. The

This article has been accepted for publication in a future issue of this journal, but has not been fully edited. Content may change prior to final publication. Citation information: DOI 10.1109/JDT.2015.2496588, Journal of Display Technology

conversion of insulating C12A7 into a conductive electride requires high temperature heat treatments and these processes should be considered while choosing a suitable OLED configuration [39].

A schematic structure of a C12A7-based OLED is shown in figure 7. Since a polycrystalline C12A7 thin film is applied on MgO single crystalline substrate, an inverted top-emitting diode, in which cathode is placed at the bottom of the device, can make the formation processes of C12A7 electride easier and allow for opaque substrates to be used. However, the application of a conventional transparent anode, such as ITO, is not simple in an inverse top organic emitting diode. The surface oxidation processes necessary for increasing the work function of the ITO anode and reducing the hole injection barrier at the organic layer-anode interface cannot be applied due to the presence of the organic material underneath the ITO film. In addition, the surface of the organic material is damaged during the sputtering of ITO. To solve these problems, an additional buffer layer with lower hole injection barrier energy, such as $Cu_{2-x}Se$, needs to be introduced between the ITO anode and the organic layer [39].

Although lowering the electron injection barrier is important in the improvement of lifetime and performance of the OLED, it is not the only determining factor in the electron transport of the device and the actual transmittance of the electrons through the interface should also be considered [39]. The electron injection barrier and possible vacuum level shift are dependent upon many parameters, such as charge transfer, chemical bonds, push-back effects, deformation of molecular dipoles, and in-gap states induced by the metallic electrode [41]. Furthermore, the work function of the cathode is dependent upon the surface structure of the material as well as the atmosphere and a minimum work function of ~2.4 eV is only obtained from a flat clean surface under ultra high vacuum [41].

The electron injection barrier energy (E_{EIB}) at the organic layer-cathode interface as a function of cathode work function is given in figure 8 for four organic materials in contact with gold (Au), silver (Ag), aluminium (Al) and C12A7:e^-. The electron injection barrier between polycrystalline C12A7:e^- thin film and tris-8-hydroxy- quinoline aluminium (Alq_3) [40] is as low as 0.6 eV, which is much lower than that of the organic layer-metallic cathode interface [39]. The electron injection barrier energy formed at single crystalline C12A7:e^--pentacene and C12A7:e^--C_{60} interfaces are 0.8 and 0.4 eV respectively. However, C12A7:e^- acts like a conventional metallic cathode with strong Fermi level pinning effect in contact with copper phthalocyanine (CuPc) [41]. It is noteworthy that the threshold voltage is affected by not only the electron injection barrier energy but also the energy of

This article has been accepted for publication in a future issue of this journal, but has not been fully edited. Content may change prior to final publication. Citation information: DOI 10.1109/JDT.2015.2496588, Journal of Display Technology

the hole injection barrier. While the applied voltage is reduced by optimising the cathode-organic layer interface, the threshold voltage is decreased by reducing the electron and hole injection barriers formed at the cathode-organic layer and anode-organic layer interfaces respectively [39].

4.3 C12A7 cathode in cold cathode fluorescent lamps

Cold cathode fluorescent lamps (CCFLs) are mainly used as backlight for liquid crystal displays (LCDs) and CCFL general lighting is proven to be more advantageous in terms of large area lighting and price when compared to LEDs. The luminescence efficiency of CCFLs is dependent upon the discharge properties of the cathode. The electron emission properties of the cathode material are controlled by the cathode surface, which in turn determines the output parameters of the device, such as the driving voltage, luminescence efficiency and energy consumption.

The operating voltage of the lamp is related to the work function of the cathode. Since the work function of C12A7 electride is lower than conventional cathode materials, such as nickel, molybdenum and tungsten , it is possible to lower the operating voltage by using C12A7:e^- [42].

The voltage necessary to sustain the discharge inside the lamp is generally lower than the applied firing voltage required to create the discharge plasma. A voltage drop near the cathode surface is partially responsible for the value of the sustaining voltage [42]. Such a voltage drop, known as the cathode fall voltage, is accompanied by the energy consumption, which is inevitable for maintaining the discharge. Since the fall voltage is related to the emission properties of the cathode and does not have an effect on emission intensity, choosing the right cathode material with a low fall voltage can improve the efficiency of the device by decreasing the energy consumption [42]. C12A7 electride has lower fall voltage in comparison to molybdenum cathode, which results in reduced energy consumption and higher efficiency. Figure 9(a) shows the superior current-voltage (I-V) characteristics of a C12A7 cathode-based lamp compared to a common molybdenum-based one with Ar/Xe discharge gas. Additional advantages include lower firing voltage and higher discharge current at a given applied voltage. C12A7 is also found to be stable against discharge plasma, sputter deposits and mercury, which is used as the source of UV emission for the phosphor [42].

This article has been accepted for publication in a future issue of this journal, but has not been fully edited. Content may change prior to final publication. Citation information: DOI 10.1109/JDT.2015.2496588, Journal of Display Technology

The stability of the lamp voltage and the luminescence intensity (brightness) over time are also determining factors in the choice of a suitable cathode material. In addition to exhibiting a good endurance (as shown in figure 9(b)), C12A7 has proven to be resistant to discharge plasma [42]. The secondary electron emission of C12A7 cathode with Xe^+ ions is higher than that of W and it gives satisfactory results as the source of UV emission, unlike other cathode materials. C12A7 cathode can, therefore, be used along with Xe as an alternative to Hg [42].

5. Conclusion

Investigations into the application of C12A7 compounds in various display devices, such as field emission displays, field-effect transistors, light emitting diodes and cold cathode fluorescent lamps have been performed. C12A7 has proven to be a suitable substitute for current commercial materials as an electron emitter as well as cathode based on laboratory results. The application of this compound as a channel layer in field-effect transistors, on the other hand, is quite complicated and requires further experiments. The main challenge regarding the development of C12A7 in a new field is understanding the characteristics of the material in a device, since it behaves quite differently in most cases due to its unique crystal structure. The application of C12A7 doped with phosphor elements has also been successful. The lifetime of a C12A7 phosphor, however, is a key factor that needs to be investigated in more detail, since the main problems in the application of efficient phosphors are limitations in brightness and endurance of conventional phosphors. Our suggestion is for C12A7 compound to be further tested in actual devices in order to obtain more accurate and practical results of the performance and efficiency of C12A7-based devices.

Acknowledgements

The first author (E.F.) is grateful to LP Displays Ltd, Blackburn, UK for partial funding of the studentship at Queen Mary, University of London. Thanks are due to Dr Lesley Hanna of Wolfson Centre for Materials Processing, Brunel University London for help in preparing the manuscript.

References

1. S. W. Kim, H. Hosono, Synthesis and properties of $12CaO \cdot 7Al_2O_3$ electride: review of single crystal and thin film growth. Philosophical Magazine Vol. 92, 19–21, 2596–2628 (2012). doi: 10.1080/14786435.2012.685770

2. J. A. McLeod, A. Buling, E. Z. Kurmaev, P. V. Sushko, M. Neumann, L. D. Finkelstein, S. W. Kim, H. Hosono, A. Moewes, Spectroscopic characterization of a multiband complex oxide: Insulating and conducting cement $12CaO{\cdot}7Al_2O_3$.*Phys. Rev. B: Condens. Matter* 85, 045204 (2012). doi: 10.1103/PhysRevB.85.045204

3. S. Matsuishi, Y. Toda, M. Miyakawa, K. Hayashi, T. Kamiya, M. Hirano, I. Tanaka, H. Hosono, High-density electron anions in a nanoporous Single Crystal: $[Ca_{24}Al_{28}O_{64}]4.(4e^-)$. *Science* **301**, 626-629 (2003)

4. Peter V. Sushko, A. L. Shluger, K. Hayashi, M. Hirano, H. Hosono, Mechanisms of oxygen ion diffusion in a nanoporous complex oxide $12CaO{\cdot}7Al_2O_3$. *Phys. Rev. B* 73, 014101 (2006). doi: 10.1103/PhysRevB.73.014101

5. R. Kiyanagi, J. W. Richardson Jr., N. Sakamoto, M. Yoshimura, Free oxygen ions and cage deformation in the nanoporous material $12CaO{\cdot}7Al_2O_3$: A temperature-dependent neutron powder diffraction study. *Solid State Ionics* 179, 2365–2371 (2008). doi:10.1016/j.ssi.2008.09.026

6. K. Hayashi, P. V. Sushko, D. Munoz Ramo, A. L. Shluger, S. Watauchi, I. Tanaka, S. Matsuishi, M. Hirano, H. Hosono, Nanoporous crystal $12CaO.7Al_2O_3$: A playground for studies of ultraviolet optical absorption of negative ions *J. Phys. Chem. B* 111, 1946-1956 (2007). Doi: 10.1021/jp065793b

7. S. Kim, S. Matsuishi, M. Miyakawa, K. Hayashi, M. Hirano, H. Hosono, Fabrication of room temperature-stable 12CaO _ 7Al2O3 electride: a review *J. Mater. Sci: Mater. Electron*. **18**, S5–S14 (2007). doi: 10.1007/s10854-007-9183-y

8. Y. Toda, Y. Kubota, M. Hirano, H. Hirayama, H. Hosono, Surface of room-temperature-stable electride $[Ca_{24}Al_{28}O_{64}]^{4+}(e^-)_4$: Preparation and its characterization by atomic-resolution scanning tunneling microscopy. *ACS nano*, Vol. 5 [3], 1907–1914 (2011)

9. Y. Toda, M. Miyakawa, K. Hayashi, T. Kamiya, M. Hirano, H. Hosono, Thin film fabrication of nano-porous 12CaO.7Al2O3 crystal and its conversion into transparent conductive films by light illumination. Thin Solid Films 445- 309–312 (2003). doi:10.1016/S0040-6090(03)01170-2

10. M. Miyakawa, Thermal conductivity and Seebeck coefficient of 12CaO·7Al2O3 electride with a cage structure. *J. Ceram. Soc. Jpn.* 117[3], 395-401 (2009). doi: 10.1103/PhysRevB.80.075201

11. S. W. Kim, Y. Toda, K. Hayashi, M. Hirano, H. Hosono, Synthesis of a room temperature stable $12CaO.7Al_2O_3$ electride from the melt and its application as an electron field emitter. *Chem. Mater. 18,* 1938-1944 (2006). doi: 10.1021/cm052367e

12. X. Liu, Y. Liu, D. Yan, H. Zhu, C. Liu, W. Liu, C. Xu, Y. Liu, H. Zhang, X. Wang, A multiphase strategy for realizing green cathodoluminescence in $12CaO{\cdot}7Al_2O_3$–$CaCeAl_3O_7$:Ce^{3+},Tb^{3+} conductive phosphor. *Dalton Trans.* 42, 16311-16317 (2013). doi: 10.1039/c3dt51958a

13. O. Gröning, O. M. Küttel, Ch. Emmenegger, P. Gröning, L. Schlapbach, Field emission properties of carbon nanotubes. J. Vac. Sci. Technol. B 18, 665 (2000). doi: 10.1116/1.591258

14. M. T. Cole, M. Nakamoto, W. I. Milne, Field emission displays (FEDs) and surface-conduction electron-emitter displays (SEDs). Handbook of Digital Imaging, Chap. 15. John Wiley & Sons, Ltd. (2015). doi: 10.1002/9781118798706.hdi023

15. Y. Toda, S. Matsuishi, K. Hayashi, K. Ueda, T. Kamiya, M. Hirano, H. Hosono, Field emission in subnanometer-sized cages in $[Ca_{24}Al_{28}O_{64}]^{4+}(4e^-)$. *Adv. Mater.* 16[8], 685-689 (2004). Doi: 10.1002/ad ma.200306484

16. M. Shiraishi , M. Ata, Work function of carbon nanotubes, Carbon Vol. 39, Issue 12, 1913–1917 (2001). doi:10.1016/S0008-6223(00)00322-5

17. T. Kamiya, S. Aiba, M. Miyakawa, K. Nomura, S. Matsuishi, K. Hayashi, K. Ueda, M. Hirano, H. Hosono, Field-induced current modulation in nanoporous semiconductor, electron-doped $12CaO.7Al_2O_3$, *Chem. Mater.*, 17[25], 6311-6316 (2005). doi: 10.1021/cm051904s

18. P. V. Sushko, A. L. Shluger, K. Hayashi, M. Hirano, H. Hosono, Localisation assisted by the lattice relaxation and the optical absorption of extra-framework electrons in $12CaO.Al_2O_3$. *Mater. Sci. Eng. C* 25, 722 – 726 (2005). doi:10.1016/j.msec.2005.06.047

19. S. W. Kim, S. Matsuishi, T. Nomura, Y. Kubota, M. Takata, K. Hayashi, T. Kamiya, M. Hirano, H. Hosono, Metallic state in a lime-alumina compound with nanoporous structure. *Nano Lett.* Vol. 7, No. 5 (2007). doi: 10.1021/nl062717b

20. M. Miyakawa, M. Hirano, T. Kamiya, H. Hosono, High electron doping to a wide band gap semiconductor $12CaO.7Al_2O_3$ thin film. *Appl. Phys. Lett.* 90, 182105 (2007) doi: 10.1063/1.2735280

21. M. Miyakawa, H. Hiramatsu, T. Kamiya, M. Hirano, H. Hosono, Fabrication and electron transport properties of epitaxial films of electron-doped12CaO _ $7Al_2O_3$ and 12SrO _ $7Al_2O_3$. *J. Solid State Chem.* 183, 385–391 (2010). doi:10.1016/j.jssc.2009.11.031

22. H. Zhu, Y. Liu, D. Yan, H. Bian, S. Li, C. Liu, C. Xu, X. Wang, Long lasting blue phosphorescence and photostimulated luminescence in $12CaO\_7Al_2O_3$:Eu thin films grown by pulsed laser deposition. *Opt. Mater.* 36, 1771–1775 (2014). doi:10.1016/j.optmat.2014.04.023

23. D. Wang, Y. X. Liu, Y. C. Liu, C. S. Xu, C. L. Shao, X. H. Li. Preparation and Visible Emission of Er-Doped 12CaO·7Al2O3 Powder. J. Nanosci. Nanotechnol., Vol. 8, No. 3, 1458–1463 (2008). doi:10.1166/jnn.2008.366

24. E. Tõldsepp, T. Avarmaa, V. Denks, E. Feldbach, M. Kirm, A. Maaroos, H. Mändar, S. Vielhauer, Synthesis and luminescence properties of Ce^{3+} doped nanoporous $12CaO\_7Al_2O_3$ powders and ceramics. *Opt. Mater.* 32, 784–788 (2010)

25. X. Liu, Y. Liu, D. Yan, H. Zhu, C. Liu, Single-phased white-emitting 12CaO.7Al2O3:Ce^{3+}, Dy^{3+} phosphors with suitable electrical conductivity for field emission displays Cite this: *J. Mater. Chem.* 22, 16839-16843 (2012). doi: 10.1039/c2jm32741d

26. H. Zhu, Y. Liu, D. Yan, X. Yan, C. Liu, C. Xu, White luminescence of Dy3+ ions doped $12CaO·7Al_2O_3$ nanopowders under UV light excitation *J. Nanosci. Nanotechnol.*, Vol. 11, No. 11, 9958-9963 (2011). doi:10.1166/jnn.2011.5291

27. Y. X. Liu, L. Mab, D. T. Yan, H. C. Zhu, X. L. Liu, H. Y. Bian, H. Zhang, X. J. Wang, Effects of encaged anions on the optical and EPR spectroscopies of RE doped C12A7. *J. Lumin.*152, 28–32 (2014)

28. D. Wang, Y. Liu, C. Xu, Y. Liu, G. Wang, X. Li, Local microstructure and photoluminescence of Er-doped $12CaO{\cdot}7Al_2O_3$ powder, *J. Rare Earth* Vol. 26, No. 3, 433-438 (2008)

29. X. L. Liu, Y. X. Liu, D. T. Yan, H. C. Zhu, C. G. Liu, C. S. Xu, Luminescence and energy transfer characteristics of Ce^{3+}- and Tb^{3+}-codoped nanoporous $12CaO{\cdot}7Al_2O_3$ phosphors. *J. Nanosci. Nanotechnol.*, Vol. 11, No. 11, 9953–9957 (2011). doi:10.1166/jnn.2011.5289

30. K. Nomura, H. Ohta, K. Ueda, T. Kamiya, M. Hirano, H. Hosono, Thin-film transistor fabricated in single-crystalline transparent oxide semiconductor. Science Vol. 300, No. 5623, 1269-1272 (2003)

31. D. Han, Y. Wang, S. Zhang, L. Sun, J. Kang, X. Liu, G. Du, L. Liu, R. Han, Fabrication and characteristics of ZnO-based thin film transistors. *9^{th} ICSICT*, 982 - 984 (2008). doi:10.1109/ICSICT.2008.4734708

32. H. S. Bae, M. H. Yoon, J. H. Kim, and S. Im, Photodetecting properties of ZnO-based thin-film transistors. *Appl. Phys. Lett.* 83, 5313-5315 (2003). doi: 10.1063/1.1633676

33. H. Hosono, Recent progress in transparent oxide semiconductors: Materials and device application. *Thin Solid Films* 515, 6000–6014 (2007). doi: 10.1016/j.tsf.2006.12.125

34. R. L. Hoffman, B. J. Norris, and J. F. Wager, ZnO-based transparent thin-film transistors. *Appl. Phys. Lett.* 82, 733-735 (2003). doi: 10.1063/1.1542677

35. S. Cherian, C. Donley, D. Mathine, L. LaRussa, W. Xia, N. Armstrong, Effects of field dependent mobility and contact barriers on liquid crystalline phthalocyanine organic transistors. *J. Appl. Phys.* Vol. 96, No. 10, 5638- 5643 (2004). doi: 10.1063/1.1803945

36. S. Park, Y. Kim, J. Han, All solution-processed high-resolution bottom-contact transparent metal-oxide thin film transistors. *J. Phys. D: Appl. Phys.* 42, 125102 (2009). doi:10.1088/0022-3727/42/12/125102

37. H. Liu, V. Avrutin, N. Izyumskaya, Ü. Özgür, H. Morkoç. Transparent conducting oxides for electrode applications in light emitting and absorbing devices *Superlattice. Microst.* 48, 458–484 (2010). doi:10.1016/j.spmi.2010.08.011

38. U. Kaufmann, M. Kunzer, K. Ko¨hler, H. Obloh, W. Pletschen, P. Schlotter, J. Wagner, A. Ellens, W. Rossner, M. Kobusch, Single chip white LEDs. *Phys.Sstat. Sol. (a)* 192, No. 2, 246–253 (2002)

39. H. Yanagi,| K. Kim, I. Koizumi, M. Kikuchi, H. Hiramatsu, M. Miyakawa, T. Kamiya, M. Hirano, H. Hosono, Low threshold voltage and carrier injection properties of inverted organic light-emitting diodes with $[Ca_{24}Al_{28}O_{64}]^{4+}(4e^-)$ cathode and Cu2-*x*Se anode. *J. Phys. Chem. C 113*, 18379–18384 (2009). doi: 10.1021/jp906386q

40. K. Kim, M. Kikuchi, M. Miyakawa, H. Yanagi, T. Kamiya, M. Hirano, H. Hosono, Photoelectron spectroscopic study of C12A7:e^- and Alq_3 interface: The formation of a low electron-injection barrier. *J. Phys. Chem. C, Vol. 111, No. 24,* 8403-8406 (2007). doi:10.1021/jp072635r

41. H. Yanagi, T. Kuroda, K. Kim, Y. Toda, T. Kamiya, H. Hosono, Electron injection barriers between air-stable electride with low work function, C12A7:e^-, and pentacene, C60 and copper phthalocyanine. *J. Mater. Chem.* 22, 4278 –4281 (2012). doi: 10.1039/c2jm14966d

42. S.Watanabe, T. Watanabe, K. Ito, N. Miyakawa, S. Ito, H. Hosono, S. Mikoshiba Secondary electron emission and glow discharge properties of $12CaO{\cdot}7Al_2O_3$ electride for fluorescent lamp applications. *Sci. Technol. Adv. Mater.* 12, 034410 (2011). doi:10.1088/1468-6996/12/3/034410

This article has been accepted for publication in a future issue of this journal, but has not been fully edited. Content may change prior to final publication. Citation information: DOI 10.1109/JDT.2015.2496588, Journal of Display Technology

Figures and tables captions

Figure 1. The structure of (a) an empty cage and (b) two neighbouring cages of C12A7

Figure 2. Logarithmic plot of electrical conductivity (σ)-electron concentration (N_e) for single crystalline bulk (Ca treatment), polycrystalline bulk (melt-solidification) and thin film (H_2+UVand oxygen-deficient amorphous top layer) of C12A7 (after [7,10, 17, 20]). Electron concentration is increased with Ca treatment time from 4 to 240 hrs.

Figure 3. The schematic illustration of a field emission display. An electrically conductive C12A7 acts as an electron emitter.

Figure 4. A comparison between the electron emission current-voltage characteristics of single crystalline and polycrystalline C12A7:e^- (after [11,15])

Figure 5. The configuration of FETs based on (a) polycrystalline C12A7:e^- thin film and (b) single crystalline C12A7:e^- bulk

Figure 6. Emission spectra of Dy^{3+} doped and Ce^{3+}, Dy^{3+} co-doped C12A7 upon excitation at λ_{ex}=362 nm (after [25])

Figure 7. Schematic structure of an OLED based on C12A7:e^- thin film as cathode

Figure 8. Energy of electron injection barrier (E_{EIB}) at the organic layer-cathode interface as a function of cathode work function (after [39, 41]). All data are obtained for single crystalline C12A7 except for C12A7-Alq_3 interface with a polycrystalline C12A7 film.

Figure 9. (a) Current-voltage characteristics of lamps with polycrystalline C12A7:e^- and molybdenum cathodes and argon (Ar)/ xenon (Xe) discharge gas and (b) endurance test results of a C12A7 cathode-based lamp (after [42]).

Table 1. Near-UV (350-420 nm) excited C12A7 phosphors along with the emission wavelengths. Major emission peaks are marked with (*).

This article has been accepted for publication in a future issue of this journal, but has not been fully edited. Content may change prior to final publication. Citation information: DOI 10.1109/JDT.2015.2496588, Journal of Display Technology

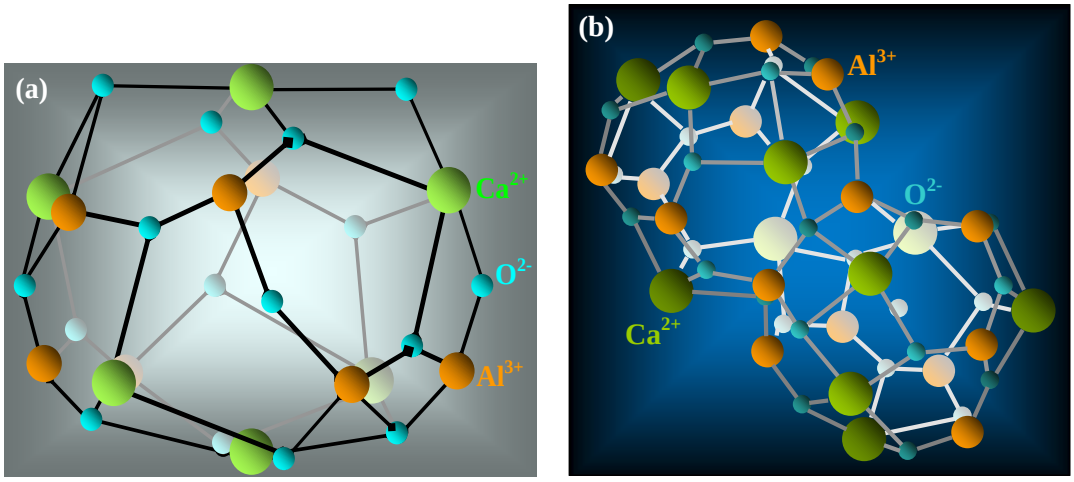

Figure 1. The structure of (a) an empty cage and (b) two neighbouring cages of C12A7

This article has been accepted for publication in a future issue of this journal, but has not been fully edited. Content may change prior to final publication. Citation information: DOI 10.1109/JDT.2015.2496588, Journal of Display Technology

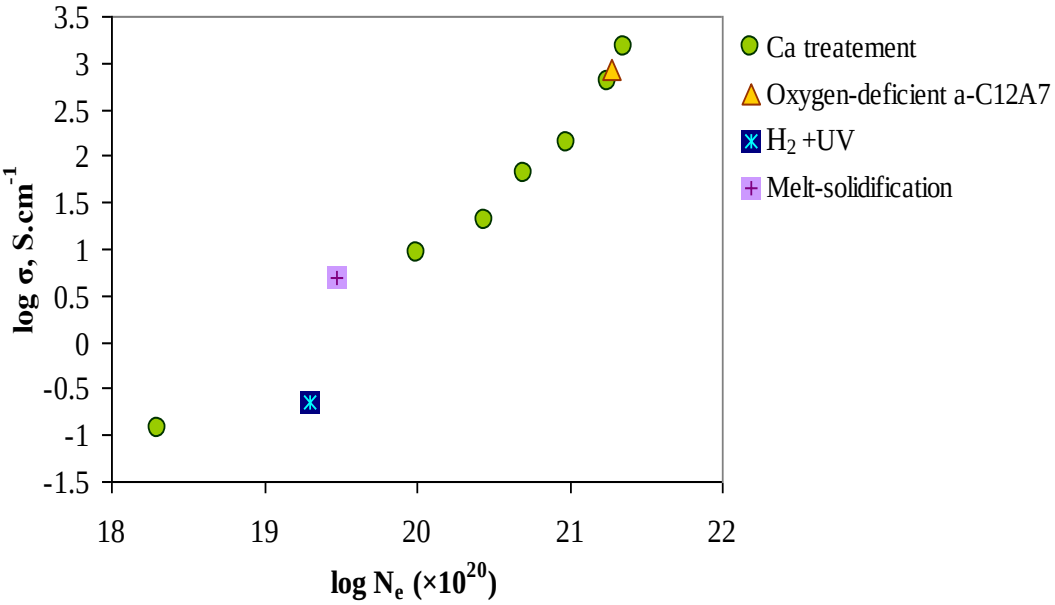

Figure 2. Logarithmic plot of electrical conductivity (σ)-electron concentration (N_e) for single crystalline bulk (Ca treatment), polycrystalline bulk (melt-solidification) and thin film (H_2+UVand oxygen-deficient amorphous top layer) of C12A7 (after [7, 10,17, 20]. Electron concentration is increased with Ca treatment time from 4 to 240 hrs.

This article has been accepted for publication in a future issue of this journal, but has not been fully edited. Content may change prior to final publication. Citation information: DOI 10.1109/JDT.2015.2496588, Journal of Display Technology

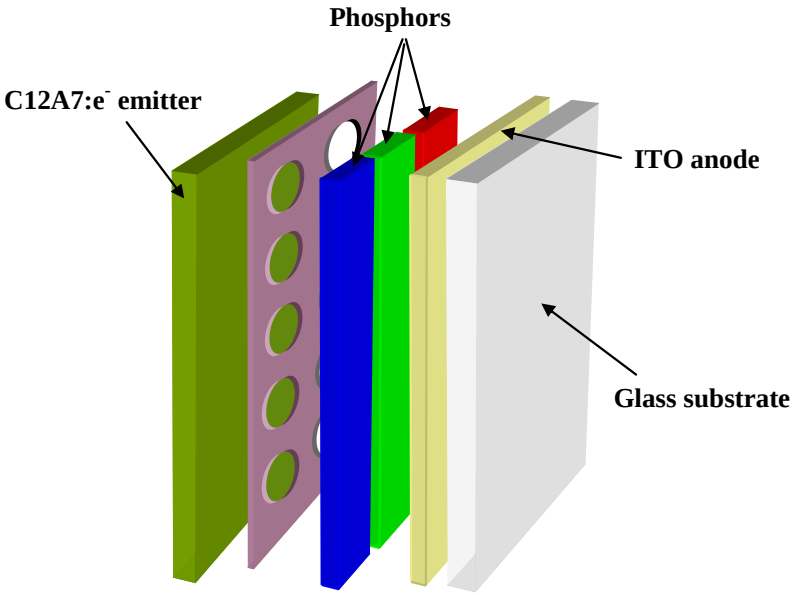

Figure 3. The schematic illustration of a field emission display. An electrically conductive C12A7 acts as an electron emitter.

This article has been accepted for publication in a future issue of this journal, but has not been fully edited. Content may change prior to final publication. Citation information: DOI 10.1109/JDT.2015.2496588, Journal of Display Technology

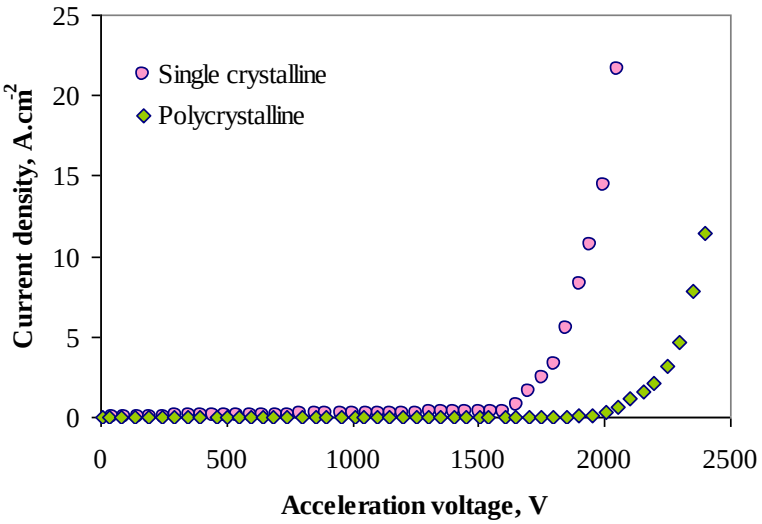

Figure 4. A comparison between the electron emission current-voltage characteristics of single crystalline and polycrystalline C12A7:e^- (after [11,15])

This article has been accepted for publication in a future issue of this journal, but has not been fully edited. Content may change prior to final publication. Citation information: DOI 10.1109/JDT.2015.2496588, Journal of Display Technology

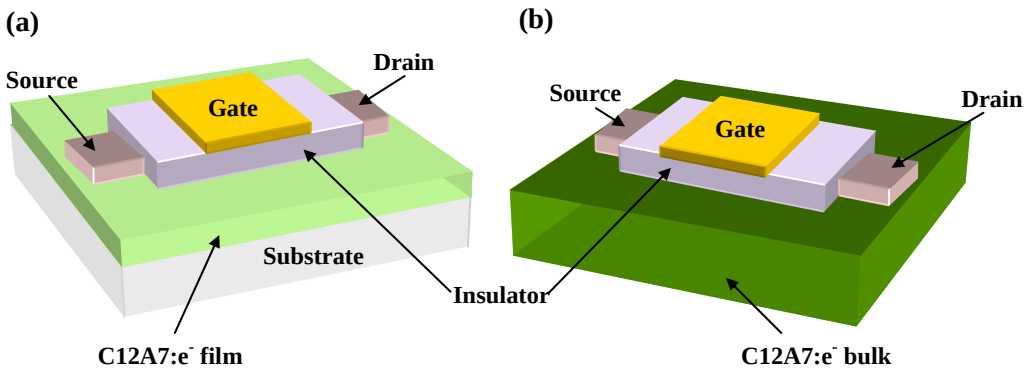

Figure 5. The configuration of FETs based on (a) polycrystalline C12A7:e^- thin film and (b) single crystalline C12A7:e^- bulk

This article has been accepted for publication in a future issue of this journal, but has not been fully edited. Content may change prior to final publication. Citation information: DOI 10.1109/JDT.2015.2496588, Journal of Display Technology

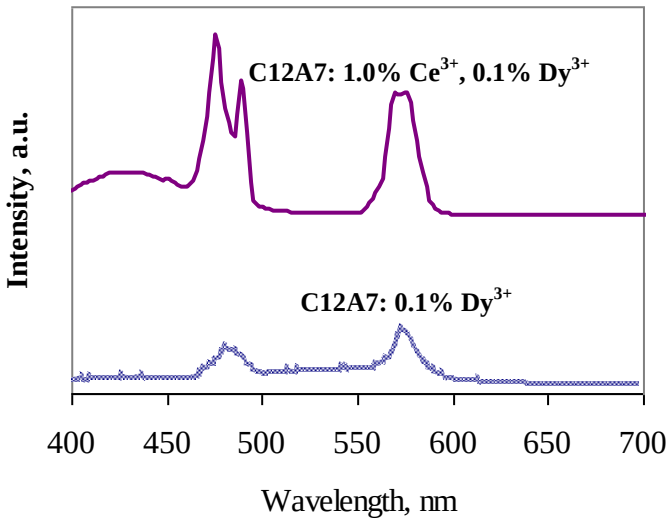

Figure 6. Emission spectra of Dy^{3+} doped and Ce^{3+}, Dy^{3+} co-doped C12A7 upon excitation at λ_{ex}=362 nm (after [25])

This article has been accepted for publication in a future issue of this journal, but has not been fully edited. Content may change prior to final publication. Citation information: DOI 10.1109/JDT.2015.2496588, Journal of Display Technology

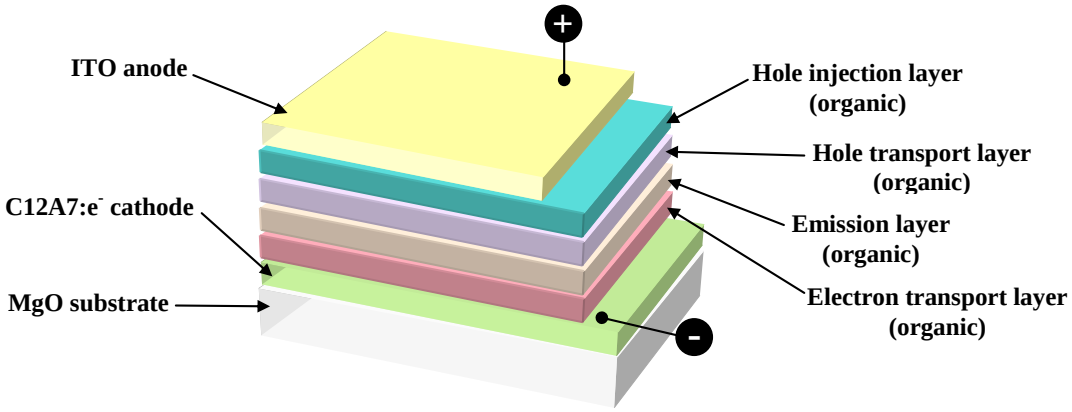

Figure 7. Schematic structure of an OLED based on C12A7:e$^-$ thin film as cathode

This article has been accepted for publication in a future issue of this journal, but has not been fully edited. Content may change prior to final publication. Citation information: DOI 10.1109/JDT.2015.2496588, Journal of Display Technology

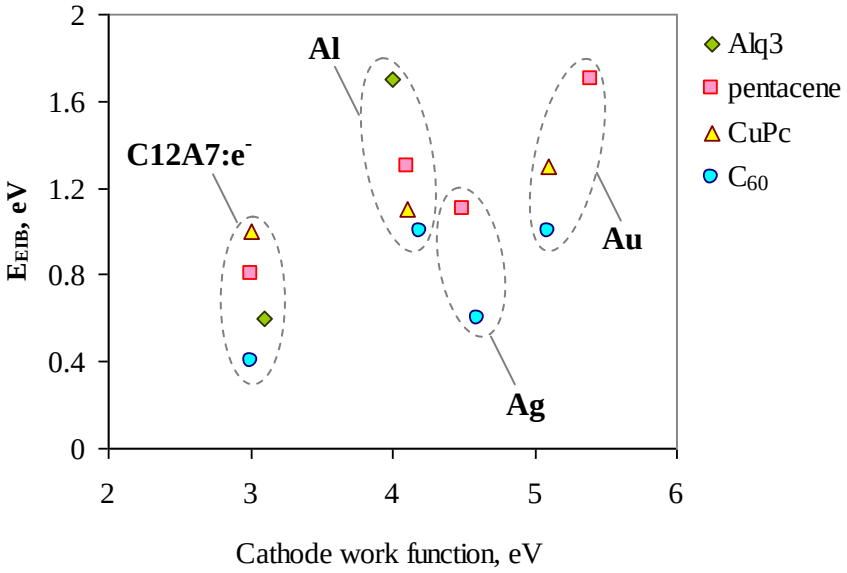

Figure 8. Energy of electron injection barrier (E_{EIB}) at the organic layer-cathode interface as a function of cathode work function (after [39, 41]). All data are obtained for single crystalline C12A7 except for C12A7-Alq_3 interface with a polycrystalline C12A7 film.

This article has been accepted for publication in a future issue of this journal, but has not been fully edited. Content may change prior to final publication. Citation information: DOI 10.1109/JDT.2015.2496588, Journal of Display Technology

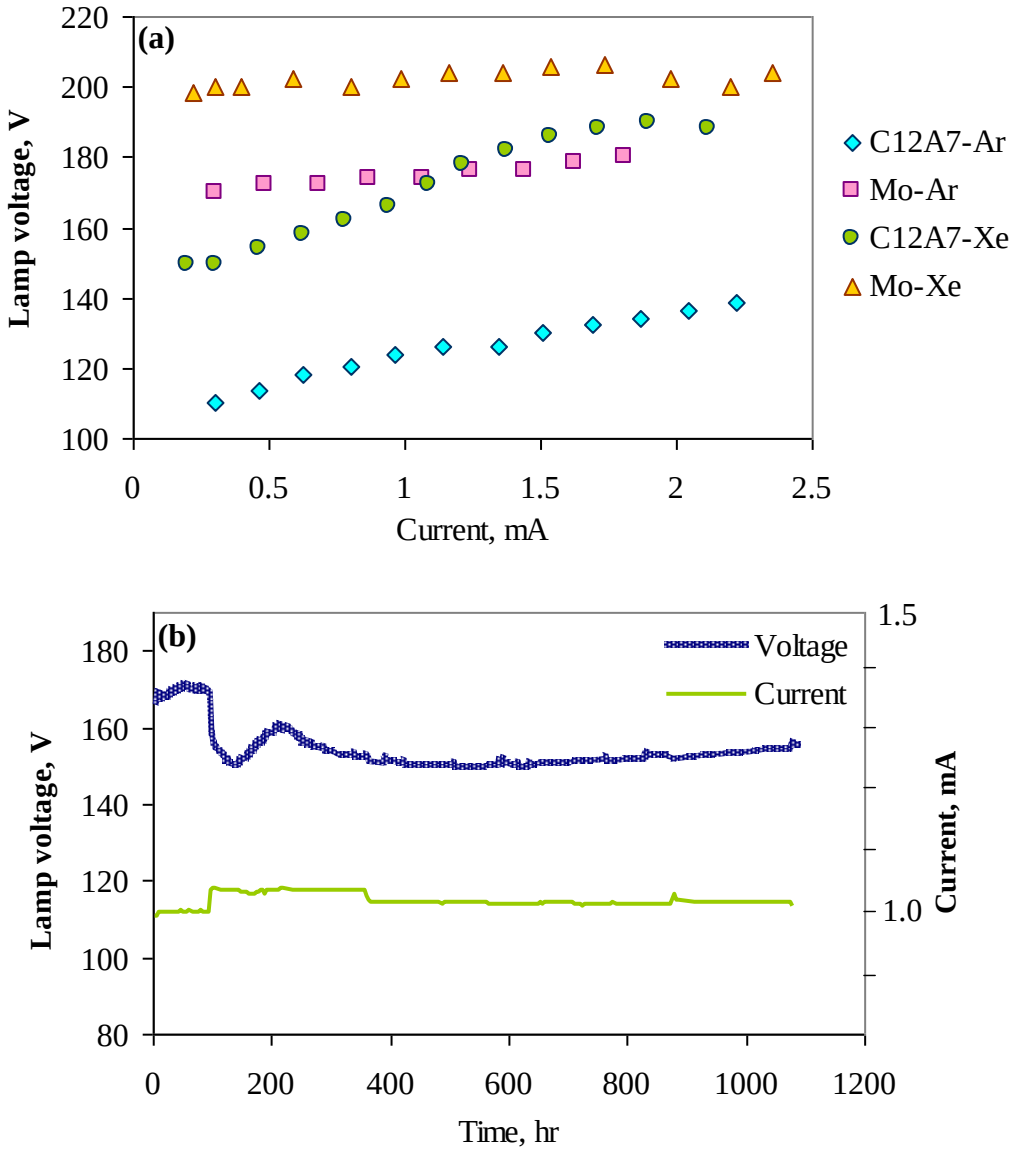

Figure 9. (a) Current-voltage characteristics of lamps with polycrystalline C12A7:e^- and molybdenum cathodes and argon (Ar)/ xenon (Xe) discharge gas and (b) endurance test results of a C12A7 cathode-based lamp (after [42]).

This article has been accepted for publication in a future issue of this journal, but has not been fully edited. Content may change prior to final publication. Citation information: DOI 10.1109/JDT.2015.2496588, Journal of Display Technology

Table 1. Near-UV (350-420 nm) excited C12A7 phosphors along with the emission wavelengths. Major emission peaks are marked with (*).

Doped Compound	*Excitation Wavelength(s), nm*	*Major Emission Wavelength(s), nm*	*Overall Emission Colour*
C12A7: Tb^{3+}	240	543 [29]	green
C12A7: Ce^{3+}	270, 350	434 [29], 463 [24]	blue
C12A7: Tb^{3+}, Ce^{3+}	350, 364	434, 543* [29]	green
C12A7-$CaCeAl_3O_7$: Tb^{3+}, Ce^{3+}	355, 364	432, 543* [12]	green
C12A7: Eu^{3+}	255	586, 616 [27]	red
C12A7: Eu^{3+}, Eu^{2+}	255	444*, 585, 615 [22]	blue
C12A7: Dy^{3+}	351	480, 571 [26]	yellowish white
C12A7: Dy^{3+}, Ce^{3+}	362	476, 576 [25]	white